SPRING REVERBERATION: A PHYSICAL PERSPECTIVE

Julian Parker, *

Dept. of Signal Processing & Acoustics,
Helsinki University of Technology
Espoo, Finland
julian.parker@tkk.fi

Stefan Bilbao,†

Acoustics & Fluid Dynamics Group,
University of Edinburgh,
Edinburgh, UK
Stefan.Bilbao@ed.ac.uk

ABSTRACT

Spring-based artificial reverberation was one of the earliest attempts at compact replication of room-like reverberation for studio use. The popularity and unique sound of this effect have given it a status and desirability apart from its original use. Standard methods for modeling analog audio effects are not well suited to modeling spring reverberation, due to the complex and dispersive nature of its mechanical vibration. Therefore, new methods must be examined.

A typical impulse responses of a spring used for reverberation is examined, and important perceptual parameters identified. Mathematical models of spring vibration are considered, with the purpose of drawing conclusions relevant to their application in an audio environment. These models are used to produce new results relevant to the design of digital systems for the emulation of spring reverberation units. The numerical solution of these models via the finite difference method is considered. A set of measurements of two typical spring reverberation units are presented.

1. INTRODUCTION

Spring reverberation was originally developed as a compact and cost-effective method of approximating room-reverberation, for use either in a studio setting or as part of musical instrument or amplification device [1, 2, 3, 4]. Although this method does produce a dense set of echoes, the peculiarities of wave propagation on a spring mean that the overall sound produced is rather different to that of a room. Nonetheless, its convenience and low-cost compared to other artificial reverberation techniques lead to widespread use in the popular music of the mid to late 20th century, with several styles of music making the sound of the spring-reverberator integral to their sonic palette. As a consequence of this use, the effect has gained a status apart from normal reverberation techniques, with an audience and specific applications of its own. With the transition of much of the music-production process to a digital environment, demand has appeared for a method of satisfactorily replicating the sound of the spring-reverberator. Early attempts at fulfilling this demand via a traditional digital reverberation approach [5] or via convolution techniques fall short for a number of reasons - notably lack of flexiblity and poor replication of the distinctive features of the effect [6]. Recently, more advanced treatments of the topic have been produced [7], which rely on calculation of a high-order all-pass filter. This method produces good results, but still has the drawback of lack of flexibility with respect to physical parameters.

This article examines the qualities that define a spring reverberation effect, relates them to theoretical models of spring vibration, and finally presents a brief overview of a method of applying these theoretical models to produce a digital algorithm for spring reverberation. A set of physical measurements of the geometry of two typical spring-reverberation units is also presented.

2. ANATOMY OF A SPRING REVERBERATION UNIT

The implementation of most spring reverberation units post-1960 is fairly standard. One or more helical springs are configured in a network. Most units consist of several springs connected in parallel, although some also utilize a number of serially connected springs in turn connected in parallel. Some less common units use springs to connect opposite ends of parallel springs, resulting in a 'Z' like configuration. The purpose of these different configurations is produce a more complex pattern of echoes.

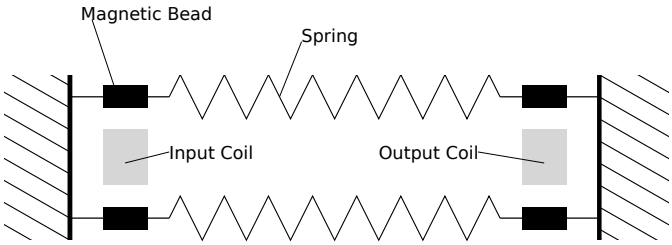

Figure 1: *Schematic diagram of a simple spring-reverberation unit, consisting of single springs connected in parallel.*

Figure 1 shows a simple schematic overview of a spring reverberation unit employing two parallel springs. Each individual spring is suspended under a small amount of tension between two sections of wire - one at each end of the casing. Attached to this section of wire is a small cylindrical magnetic bead. The wire then passes through a section of rubber damping material before terminating in a soldered connection to the casing of the device. The magnetic bead is driven torsionally by passing a signal into a nearby electromagnetic coil. Torsional vibration of the magnet/wire system translates to vibration tangential to the path of the wire at a point within the helix. At the opposite end of the spring, the other section of straight wire also has a magnetic bead attached. The vibration of the magnetic bead induces a current in a nearby

* This work was supported by the Academy of Finland (project no. 122815)

† This work was supported by the Engineering and Physical Sciences Research Council UK, under grant number C007328/1

coil, and an output signal is therefore produced. The system is essentially symmetrical, although the input and output coils tend to be wound differently so as to provide appropriate input and output impedances. Input and output to multiple springs can be handled by a single pair of coils by extending the core of the electromagnet.

3. ANALYSIS OF A TYPICAL IMPULSE RESPONSE

A spectrogram of the initial section of a typical single-spring impulse response can be seen in Figure 2. Clearly visible are a number of echoes, the form of which indicates highly dispersive behaviour. There appear to be two distinct regions within the impulse response, a region of lower-frequency dispersive echoes and a region of high-frequency (and less dispersive) echoes. The high-frequency echoes appear to repeat at a faster rate than the low-frequency echoes. The transition point between these two regions is labelled as F_C, and appears to correspond with a point of minimum propagation velocity.

In the majority of springs measured, the region of high frequency echoes above F_C is of much lower amplitude than that of the echoes below F_C, therefore it would seem reasonable to assume that the characteristic sound of a spring reverberator is mainly related to the region below F_C. The nature of these echoes can be described by two parameters - the transition frequency F_C, and the time between each echo, T_D.

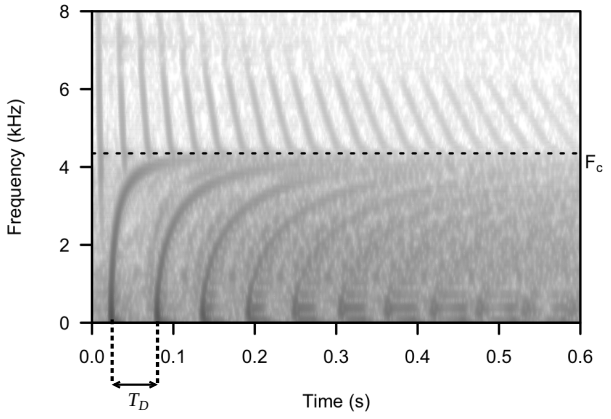

Figure 2: *Spectrogram of measured impulse response of a typical spring (see Table 2, Spring 3).*

4. HELICAL SPRING VIBRATION MODELS

Mathematical modeling of spring vibration is a topic which has seen much work over the years, mainly due to its importance in mechanical engineering. Some of the earliest models treat a spring as a uniform elastic bar [8], but such models do not reproduce the dispersion characteristics which make a spring interesting in an audio context [6]. To reproduce these characteristics, it appears to be necessary to model the helical geometry of the spring. The best known of these helical models is the work of Wittrick [9], written as a system in twelve variables. The Wittrick model has also been extended to account for loading of the spring [10].

Fletcher et al [11, 12] make a number of approximations which allow them to present a simpler model than Wittrick's system. Firstly, they assume that the helix angle of the spring will be small enough to be considered to be zero. This essentially reduces the problem to one of a curved rod and allows them to consider only vibrations in the plane of curvature. The effect of neglecting the helix angle removes the need to consider torsional motion, and hence Timoshenko effects. The governing equations they produce are as follows:

$$\frac{\partial^2 u}{\partial t^2} = \frac{E}{\rho}\left(\frac{\partial^2 u}{\partial s^2} - \kappa\frac{\partial v}{\partial s}\right) \tag{1a}$$

$$\frac{\partial^2 v}{\partial t^2} = -\frac{Er^2}{4\rho}\left(\frac{\partial^4 v}{\partial s^4} + 2\kappa^2\frac{\partial^2 v}{\partial s^2} + \kappa^4 v\right) + \frac{E\kappa}{\rho}\left(\frac{\partial u}{\partial s} - \kappa v\right) \tag{1b}$$

where E is Young's modulus for the material of the wire, ρ is the density of the material, r is the radius of the wire and κ is the curvature of the helix. u gives displacement in the direction of the tangent of the helix at any point, v gives displacement in the direction of the radius of curvature. s is a coordinate that follows the line of the wire. When $\kappa = 0$, system (1) reduces to the equation of motion of an ideal bar (in v), and the 1D wave equation (in u). Figure 3 shows the direction of the displacements u and v with respect to the geometry of the spring.

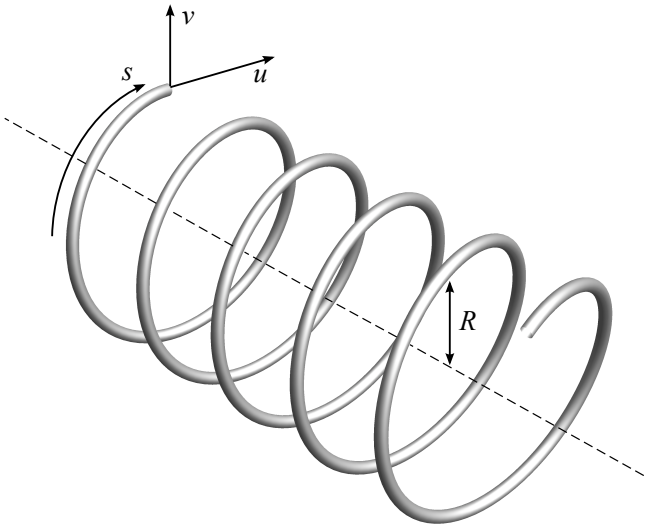

Figure 3: *Section of helical spring showing the direction of the displacements u and v, both of which are dependent on the helix arc-length coordinate, s. Also shown is the helix radius, R.*

This system is linear and shift-invariant, and therefore its characteristics may be summarized by a dispersion relation, i.e. the relationship of spatial frequency (wavenumber, β) to temporal frequency (f). The dispersion relation possesses four solutions grouped in two pairs, corresponding to two modes of oscillation. One of these modes is beyond the range of human hearing [6, 13]. The other mode is within human hearing range, and its form is given in Figure 4.

The form of the dispersion relation clearly shows the behaviour observed in the impulse response in Figure 2. The derivative of the dispersion relation gives the group velocity, a measure of the

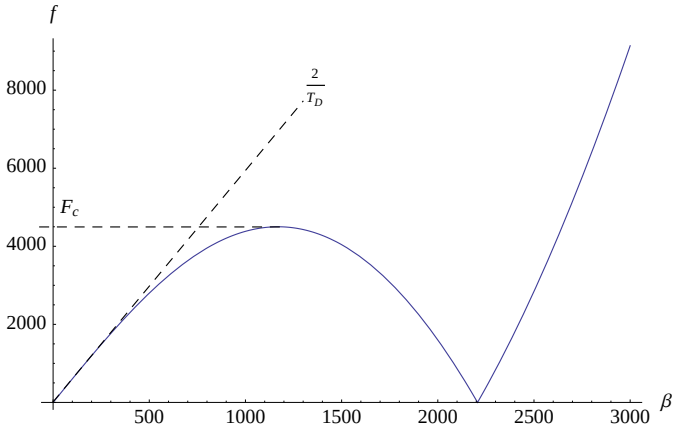

Figure 4: *Dispersion relation of audio-range mode calculated from Fletcher model for a typical spring (see Table 2, Spring 3).*

speed of propagation of a disturbance through the system around a particular wavenumber. The local maximum in the dispersion relation therefore corresponds with a point of minimum propagation velocity. It is clear from the dispersion relation that this point corresponds with the transition frequency F_C observed in the impulse response.

It is important to notice that the dispersion relation for this system is not a single-valued function of frequency. In the range of frequencies below F_C, there are three different propagation velocities associated with a particular frequency. This could potentially make a spring-reverberation model constructed via standard signal processing constructs more complex and more computationally demanding, as multiple parallel processing paths would be necessary. It is therefore beneficial to consider a different approach, one based on direct numerical solution of system (1) - with the eventual goal of comparison with an equivalent model constructed via the standard audio signal processing paradigm.

If system (1) is to be used for numerical modeling of a spring reverberator, some form of loss must be incorporated. In the absence of more detailed insight into the loss mechanisms of the real system, it is possible to add an ad-hoc loss model. This is achieved simply by adding loss terms of $-2\sigma_x \frac{\partial x}{\partial t}$ to each equation, where x represents the variable in question. It is also necessary to model the input/output process accurately, and this is achieved by coupling a mass-spring system to each end of the spring to represent the magnetic driving method[13].

4.1. Characterizing Perceptual Properties in Terms of Physical Parameters

By manipulation of the dispersion relation for the system 1, it is possible to derive some results connecting the perceptual parameters, F_C and T_D, to easily measurable physical parameters of the spring.

$$T_D \approx \frac{4LR}{r\sqrt{\frac{E}{\rho}}} \tag{2}$$

where L is the uncurled length of the wire, R is the radius of the helix, r is the radius of the wire, ρ is the density of the material and E is Young's modulus of the material. T_D gives a measure of the delay time of the spring, specifically the time taken for a wave to propagate the length of the spring twice, in the limit as $\beta \to 0$. This gives a measure of the time between discrete echoes in the impulse response. The limit as $\beta \to 0$ is chosen, as this is the point of maximum propagation velocity within the low-frequency dispersive region. As should be clear from the geometry, L can be calculated from more easily measured parameters as follows:

$$L = \sqrt{(2\pi RN)^2 + H_L^2} \tag{3}$$

where R is the radius of the helix, H_L is its length and N is the number of turns completed over the course of its length.

An expression for the transition frequency F_C can also be derived:

$$F_C \approx \frac{3r\sqrt{\frac{E}{\rho}}}{16\sqrt{5}\pi R^2} \tag{4}$$

These two results relate the main perceptual features of a single-spring reverberator to physical measurements of the spring, and hence may be used to both predict the response of real springs and as a more intuitive physical parameter model for models based on signal processing constructs. A discussion of the derivations of the above results is given in Appendix B.

5. FINITE DIFFERENCE MODELS

A standard approach to simulation that is especially suited to problems in 1D is to make use of a finite difference approximation. System (1) is a coupled pair of equations in 1D, and is therefore a good candidate for solution using this method.

There are numerous well known approaches to constructing a finite difference approximation to a continuous system. A conceptually simple and flexible approach is to define discrete approximations to differential operators, known as difference operators [14, 13], along with discrete versions of the dependent variables of the system, known as grid functions. An analogous discrete system can then be prodeced by replacing differential operators with difference operators and dependent variables with grid functions. The difference operators are defined in terms of unit delays (for time differentials) or unit shifts (for spatial differentials), and therefore this discrete system can be expanded out into a scheme for calculation of a numerical solution to the system. It is important to note that it is possible to construct many different difference operators for a particular differential operator. For example, it is possible to construct $\frac{\partial}{\partial x}$, an approximation to a first differential with respect to some spatial coordinate x, in terms of forward shifts, backwards shifts or a mixture of the two. As a consequence, many calculation schemes varying in robustness and accuracy can be produced from a single discrete system.

Selection of only centered difference operators results in an explicit calculation scheme [6]. However, the scheme produced has severe stability and accuracy problems, producing acceptable results only at very high sampling frequencies. A more advanced approach is to specify an implicit family of schemes, via the use of the relationship between certain difference operators and a similarly defined discrete averaging operator [14, 13]. The result is a family of schemes with a number of free parameters, which can then be tuned to produce optimum stability and accuracy. The results produced by this approach are much better than those produced by the naive explicit approach.

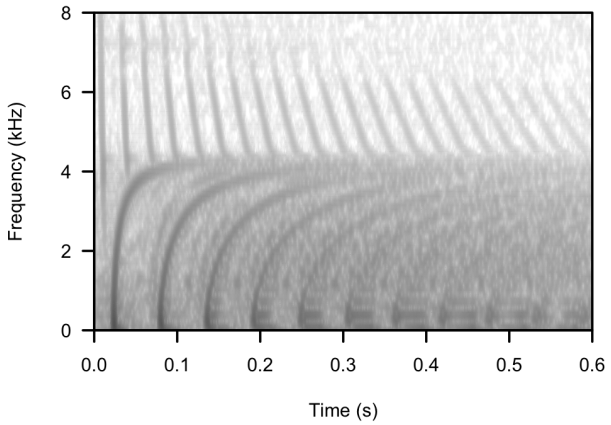

Figure 5: *Spectrogram of impulse response of a typical spring (for measurements see Table 2, Spring 3).*

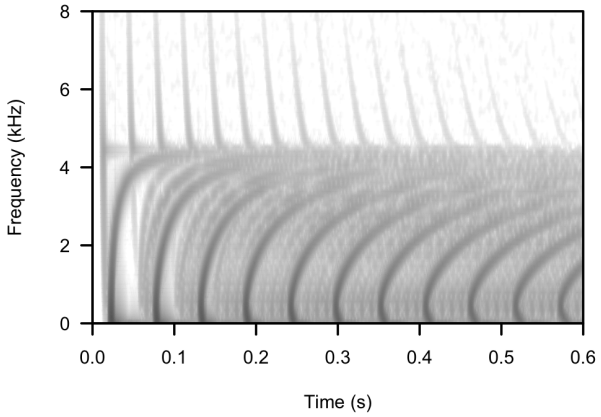

Figure 6: *Spectrogram of impulse response of simulation of a typical spring (for measurements see Table 2, Spring 3).*

Figure 5 shows a spectrogram of the impulse response of a spring of the measurements given for Spring 3 in Table 2. Figure 6 shows a spectrogram of a simulation of this spring via the use of the implicit family of schemes described above. Clearly, the agreement between the measured response and the simulated response is quite close. The values of T_D and F_C both appear to be in good agreement. However, the reflection rate of echoes in the region above F_C in the simulated result appears to be lower than that of the real result. This is consistent with the increasing effect of numerical dispersion at higher frequencies[13]. The importance of the discrepancy is debatable, as the perceptual importance of the region above F_C is lower than that of the region below. It may be possible to remove this discrepancy with further tuning of the free parameters of the implicit family of schemes.

5.1. Viability as a method for real-time audio processing

Consideration of the computational complexity of this approach is important [13]. The memory cost and number of operations required per time step scale roughly linearly with T_D and F_C, and roughly with the square root of the sampling frequency. An un-optimised implementation of the scheme in MATLAB running under a Microsoft Windows environment and using a single-core 2GHz Intel processor takes approximately one minute to calculate a three second sample at a sample rate of 44100 Hz. The parameters chosen were consistent with those given in Appendix A. This is rather far from real-time operation, but gains can likely be made by optimizing the scheme and implementing in a more efficient environment.

6. CONCLUSIONS

Mathematical models of helical vibration provide a useful insight into spring reverberation, and can be used to produce novel expressions relating physical parameters of the spring with the perceptual qualities of its sound. Numerical solution of these models via finite difference techniques shows some promise for implementation in audio applications, but requires more development to improve numerical accuracy and reduce computational cost to the level required for real-time application.

7. REFERENCES

[1] L. Hammond, "Electrical musical instrument," US Patent No. 2230836, February 1941.

[2] L. Hammond and J.M. Hanert, "Electrical musical instrument," Feb. 25 1941, US Patent 2,233,258.

[3] H. Laurens, "Musical instrument," Nov. 11 1941, US Patent 2,262,179.

[4] J.D. Stack, "Sound reverberating device," Mar. 9 1948, US Patent 2,437,445.

[5] R. Kuroki, "Sound effect imparting apparatus ," Jan. 26 1999, US Patent 6,580,796.

[6] J.D. Parker, "Spring reverberation: A finite difference approach," M.S. thesis, University of Edinburgh, 2008.

[7] J.S. Abel, D.P. Berners, S. Costello, and J.O. Smith III, "Spring reverb emulation using dispersive allpass filters in a waveguide structure," *AES 121st Int'l Conv., San Francisco*, 2006.

[8] J.A. Haringx, *On Highly Compressible Helical Springs and Rubber Rods, and Their Application for Vibration-Free Mountings*, Philips Research Laboratories, 1950.

[9] W.H. Wittrick, "On elastic wave propagation in helical springs," *International Journal of Mechanical Sciences*, 1966.

[10] L.E. Becker, G.G. Chassie, and W.L. Cleghorn, "On the natural frequencies of helical compression springs," *International Journal of Mechanical Sciences*, vol. 44, no. 4, pp. 825–841, 2002.

[11] N.H. Fletcher, T. Tarnopolskaya, and F.R. de Hoog, "Wave propagation on helices and hyperhelices: a fractal regression," *Proceedings: Mathematics, Physical and Engineering Sciences*, pp. 33–43, 2001.

[12] T. Tarnopolskaya, F.R. de Hoog, and N.H. Fletcher, "Low-frequency mode transition in the free in-plane vibration of curved beams," *Journal of Sound and Vibration*, vol. 228, no. 1, pp. 69–90, 1999.

[13] S. Bilbao and J.D. Parker, "A virtual model of spring reverberation," *IEEE Transactions on Audio, Speech and Language Processing*, Accepted.

[14] S. Bilbao, *Numerical Sound Synthesis*, John Wiley and Sons, 2009.

[15] A. Farina, "Simultaneous measurement of impulse response and distortion with a swept-sine technique," *Preprints - Audio Engineering Society*, 2000.

A. SPRING MEASUREMENTS

This appendix presents a set of measurements of spring geometries taken from two typical spring reverberation units. Measurements were taken using a micrometer and Vernier calipers, and are reasonably accurate - however the intention is to provide an idea of the geometries typical to a spring reverberation unit rather than definitive measurements of a particular unit.

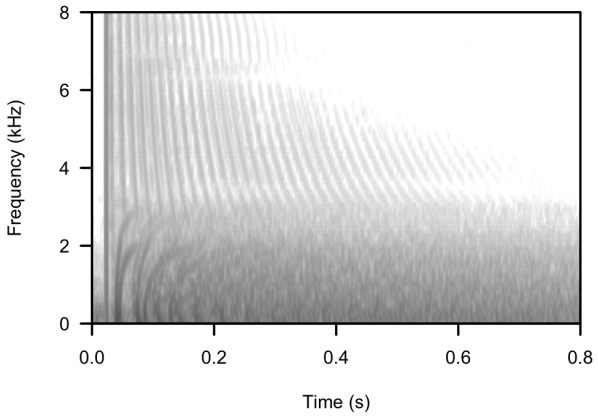

Figure 7: *Spectrogram of impulse response of Olson X-82 reverb unit.*

The X-82 is a small device from the early 1960s, manufactured by Olson Electronics. It consists of two small springs in parallel, and according to the manufacturer's literature it is intended for use in small instrument amplifiers or in a car audio system. The spring geometries appear to have been chosen so as to provide similar T_D for each spring, but with a differing F_C.

The second unit is a device taken from a Leem Pro KA-1210 guitar amplifier from the early 1990s. It is slightly larger than the Olson unit, and employs three springs in parallel. In contrast to the design of the Olson unit, this unit uses spring geometries chosen to provide a range of T_D values but very similar F_C values.

Both units appear to use steel wiring, and therefore a Young's Modulus of $E = 2^{11} N/m^2$ and a density of $\rho = 7800\ kg/m^3$ are used for all the calculations in this document.

Impulse response measurements were taken of these two units, using a sine-sweep method [15]. Spectrograms of the response of both units are given in figures 7 and 8. The impulse responses of each individual spring was measured by damping the other springs within the unit using padded clamps. Further information, including impulse responses for each individual spring and further documentation of the units, is available at:
`http://www.acoustics.hut.fi/publications/papers/dafx09-sr/`

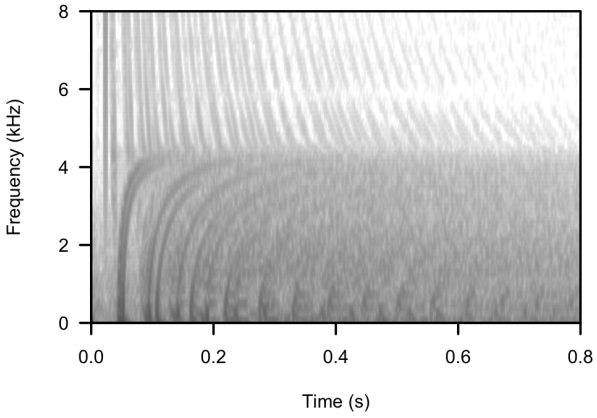

Figure 8: *Spectrogram of impulse response of Leem Pro KA-1210 reverb tank.*

Table 1: *Olson X-82 Measurements*

	Spring 1	Spring 2
Helix Length (cm)	6.5	6.5
Helix Diameter (cm)	0.54	0.61
Number of Turns	148	133
Wire Diameter (cm)	0.035	0.035
Magnet Length (cm)	0.5	0.5
Magnet Diameter (cm)	0.21	0.21

B. DERIVATION OF PERCEPTUAL PARAMETERS

In order to derive the perceptual parameters discussed in section 4.1, we start by examining the dispersion relation of system 1. The dispersion relation is produced by writing the system in matrix representation, inserting a test solution of the form $e^{st+i\beta x}$, and calculating the determinant of the matrix.

$$\begin{aligned} &\frac{\mathrm{E}^2 r^2 \beta^2}{4L^2 R^4 \rho^2} - \frac{\mathrm{E}^2 r^2 \beta^4}{2L^4 R^2 \rho^2} + \frac{\mathrm{E}^2 r^2 \beta^6}{4L^6 \rho^2} \\ &\quad - \frac{\mathrm{E} r^2 \omega^2}{4R^4 \rho} - \frac{\mathrm{E}\omega^2}{R^2 \rho} - \frac{\mathrm{E}\beta^2 \omega^2}{L^2 \rho} \\ &\quad + \frac{\mathrm{E} r^2 \beta^2 \omega^2}{2L^2 R^2 \rho} - \frac{\mathrm{E} r^2 \beta^4 \omega^2}{4L^4 \rho} + \omega^4 \quad = 0 \end{aligned} \tag{5}$$

where ω and β are the angular frequency and wavenumber respectively, E is Young's modulus of the material, ρ is the density of the material, L is the uncurcled length of the wire, r is the radius of the wire and R is the radius of the helix. Solving this equation for ω produces two pairs of solutions, only one of which it is necessary to consider (see section 4). The group velocity can be calculated as a function of β by differentiating this solution with respect to β. If we evaluate the limit of the group velocity as $\beta \to 0$, we produce the following expression:

$$\nu_0 = \frac{\sqrt{\frac{E}{\rho}} r}{LR\sqrt{4 + \frac{r^2}{R^2}}}$$

Table 2: *Leem Pro KA-1210 Measurements*

	Spring 1	Spring 2	Spring 3
Helix Length (cm)	16.3	16.3	16.3
Helix Diameter (cm)	0.44	0.45	0.46
Number of Turns	303	280	351
Wire Diameter (cm)	0.035	0.035	0.035
Magnet Length (cm)	0.4	0.4	0.4
Magnet Diameter (cm)	0.15	0.15	0.15

Since $\frac{r^2}{R^2}$ is of the order of 10^{-4} for values of the parameters typical to our application, we can make the following approximation:

$$\nu_0 \approxeq \frac{\sqrt{\frac{E}{\rho}}r}{2LR}$$

Given that the system is dimensionless and defined over the unit interval, we need only take the reciprocal in order to derive an approximate expression for the time taken to traverse the length of the spring once. The time between two echoes received at the output end of the spring is clearly equivalent to the time taken to traverse the length of the spring twice, hence we can produce an expression for this delay time:

$$T_D \approxeq \frac{4LR}{r\sqrt{\frac{\mathrm{E}}{\rho}}}$$

To derive the parameter F_C, the dispersion relation given in equation 5 is again solved, and the relevant solution evaluated at the point $\beta = q/2$. After some manipulation and a Taylor expansion, we arrive at:

$$F_C \approxeq \frac{3r\sqrt{\frac{\mathrm{E}}{\rho}}}{16\sqrt{5}\pi R^2}$$

which is accurate to first order.